

## Biophysical Letter

# Decoding Cytoskeleton-Anchored and Non-Anchored Receptors from Single-Cell Adhesion Force Data

Ediz Sariisik,<sup>1,2,3</sup> Cvetan Popov,<sup>1</sup> Jochen P. Müller,<sup>2</sup> Denitsa Docheva,<sup>1,3</sup> Hauke Clausen-Schaumann,<sup>2,3</sup> and Martin Benoit<sup>2,3,\*</sup>

<sup>1</sup>Experimental Surgery and Regenerative Medicine, Department of Surgery and <sup>2</sup>Center for NanoScience, Ludwig-Maximilians-Universität München, Munich, Germany; and <sup>3</sup>Center for Applied Tissue Engineering and Regenerative Medicine, University of Applied Sciences, Munich, Germany

**ABSTRACT** Complementary to parameters established for cell-adhesion force curve analysis, we evaluated the slope before a force step together with the distance from the surface at which the step occurs and visualized the result in a two-dimensional density plot. This new tool allows detachment steps of long membrane tethers to be distinguished from shorter jumplike force steps, which are typical for cytoskeleton-anchored bonds. A prostate cancer cell line (PC3) immobilized on an atomic-force-microscopy sensor interacted with three different substrates: collagen-I (Col-I), bovine serum albumin, and a monolayer of bone marrow-derived stem cells (SCP1). To address PC3 cells' predominant Col-I binding molecules, an antibody-blocking  $\beta$ 1-integrin was used. Untreated PC3 cells on Col-I or SCP1 cells, which express Col-I, predominantly showed jumps in their force curves, while PC3 cells on bovine-serum-albumin- and antibody-treated PC3 cells showed long membrane tethers. The probability density plots thus revealed that  $\beta$ 1-integrin-specific interactions are predominately anchored to the cytoskeleton, while the nonspecific interactions are mainly membrane-anchored. Experiments with latrunculin-A-treated PC3 cells corroborated these observations. The plots thus reveal details of the anchoring of bonds to the cell and provide a better understanding of receptor-ligand interactions.

Received for publication 27 January 2015 and in final form 22 July 2015.

\*Correspondence: [martin.benoit@physik.uni-muenchen.de](mailto:martin.benoit@physik.uni-muenchen.de)

This is an open access article under the CC BY-NC-ND license (<http://creativecommons.org/licenses/by-nc-nd/4.0/>).

Atomic-force-microscopy-based, single-cell force spectroscopy is widely used to study cell mechanics and cell adhesion (1). Environmental changes influencing the cellular behavior are frequently in focus during such investigations (2–4). Force distance curves from single-cell force spectroscopy contain far more information than just absolute force values, and moreover, quantify the underlying molecular interactions of cell surface receptors with their respective substrates (5); the receptors are embedded in a complex cellular environment, and the force distance curves also contain valuable information about the anchoring of the receptors to the plasma membrane or the cytoskeleton.

Here we have investigated the interaction between the prostate cancer cell line (PC3) and collagen (Col-1) (Fig. 1) as well as monolayers of the Col-I-expressing mesenchymal stem cell line (SCP1) (see the Supporting Material and Sariisik et al. (6) for experimental details). Because quantitative polymerase chain reaction revealed high expression levels of the collagen binding integrins  $\alpha$ 1 $\beta$ 1 and  $\alpha$ 2 $\beta$ 1 in PC3 cells ( $0.08 \pm 0.01$  and  $0.31 \pm 0.1$ -fold of the GAPDH expression; see Popov et al. (7) for details), we used a  $\beta$ 1-integrin blocking antibody (monoclonal antibody to CD29; Acris Antibodies, San Diego, CA) to identify the specific contribution of these integrins. A bovine serum albumin

(BSA)-coated surface and latrunculin-A-treated PC3 cells were used as additional negative controls (7).

To begin, the commonly derived parameters to quantify cell adhesion—the adhesion rate, the number of steps per curve, the detachment force, the dissipated work, and the step height—were analyzed (see Benoit and Selhuber-Unkel (8) and the Supporting Material). On Col-I-coated surfaces and on the SCP1 monolayer, the adhesion rate and the number of steps are found to be significantly higher than on BSA-coated surfaces, where both parameters are in the same range as for the antibody-treated PC3 cells (see Fig. 2 A). The same trend can be observed for the detachment force and dissipated work, while the step height shows much less variation (data not shown). However, despite a clear difference in four of the parameters quantifying the interactions, no information about the type of interaction—and in particular about the anchoring of the relevant receptors to their respective microenvironment—can be obtained from any of these parameters alone. To gain more

Editor: Andreas Engel.

© 2015 The Authors

<http://dx.doi.org/10.1016/j.bpj.2015.07.048>



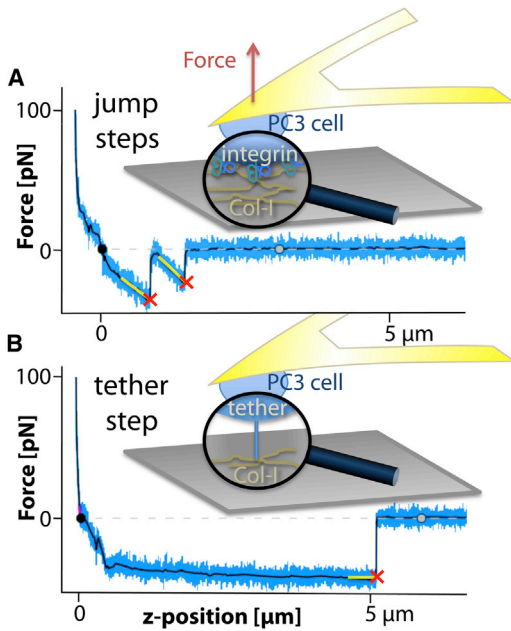


**FIGURE 1** Two force traces of a PC3 cell separated from a Col-I substrate at a velocity of  $3 \mu\text{m/s}$  after contacts of  $0.3 \text{ s}$  at  $100 \text{ pN}$ . (Crosses) Steps. (Black line) Smoothed force trace. A line-fit indicates the slope before a step. (A) Jumplike steps were defined at slopes  $< -10 \text{ pN}/\mu\text{m}$ . (B) Tetherlike steps, caused by membrane tubes pulled from the cell by bonds not anchored to the cytoskeleton, typically show slopes of  $0 \pm 10 \text{ pN}/\mu\text{m}$ . To see this figure in color, go online.

detailed insight into the receptor anchoring to the cell membrane or cytoskeleton, we extracted two additional parameters from the data and displayed them in normalized

two-dimensional probability density maps: the position of detachment force steps (distance from the contact point), and the slope before each step.

Interactions involving receptors linked to the cytoskeleton typically exhibit a clear rise in force just before the unbinding event, like in the force curve displayed in Fig. 1 A (2). On the other hand, long plateaus with slopes around zero, as displayed in Fig. 1 B, are typical of tethers being pulled out of the cell membrane. Here the constant force before the unbinding event is caused by the constant tension of the plasma membrane (8–10).

We evaluated the step position using the step detection algorithm developed by Opfer and Gottschalk (11) and the slope using a linear fit starting  $500 \text{ nm}$  before each force step (6). Fig. 2, B and C, shows histograms of the position and slope. In Fig. 2 D, both parameters are combined in a color-coded, two-dimensional probability density plot (i.e., the two-dimensional plot). As can be seen from this two-dimensional plot of PC3 cells on Col-I, there are two distinct regions: one at step positions between  $0.5$  and  $1 \mu\text{m}$  and slopes at  $\sim -30 \text{ pN}/\mu\text{m}$ , pointing to membrane-linked cellular receptors; and a second one at  $\sim 3 \mu\text{m}$  and slopes close to  $0 \text{ pN}/\mu\text{m}$ , which represents membrane tethers.

Fig. 3 shows slope-versus-step-position plots of interactions of PC3 cells (and antibody-treated PC3 cells) with Col-I- and BSA-coated substrates as well as with SCP1 monolayers. As already mentioned, on the Col-I-coated substrate (Fig. 3 A is identical to Fig. 2 D), there are two distinct peaks—one that resembles interactions of cytoskeleton-linked receptors (jumps), and one that resembles membrane tethers. Without antibody blocking of  $\beta 1$ -integrin, the

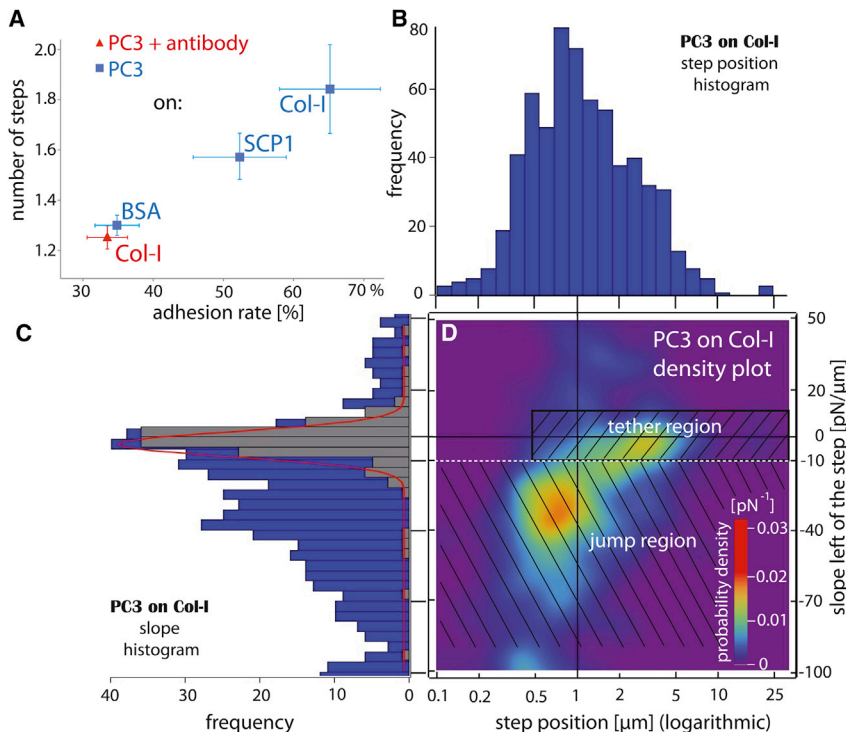


**FIGURE 2** (A) Number of steps versus adhesion rate reveals that PC3 cells after antibody treatment interact nonspecifically, like on BSA. For each probed interaction, 10 different cells with at least 100 force traces each were measured. Standard errors are given as error bars. (B) Histogram of the step positions and (C) corresponding slopes of untreated PC3 cells on collagen substrate. (Gray subsection) Membrane tethers (Gaussian fitted on top). (D) A smoothed two-dimensional probability density plot of the slope versus step position reveals cumulated jumps and a few longer tethers. (Black lines) Zero slope and  $1 \mu\text{m}$  step position. (White line at  $-10 \text{ pN}/\mu\text{m}$ ) Apparent best border between tether region and jump region. (Inset, colored bar codes for the probability densities.) To see this figure in color, go online.

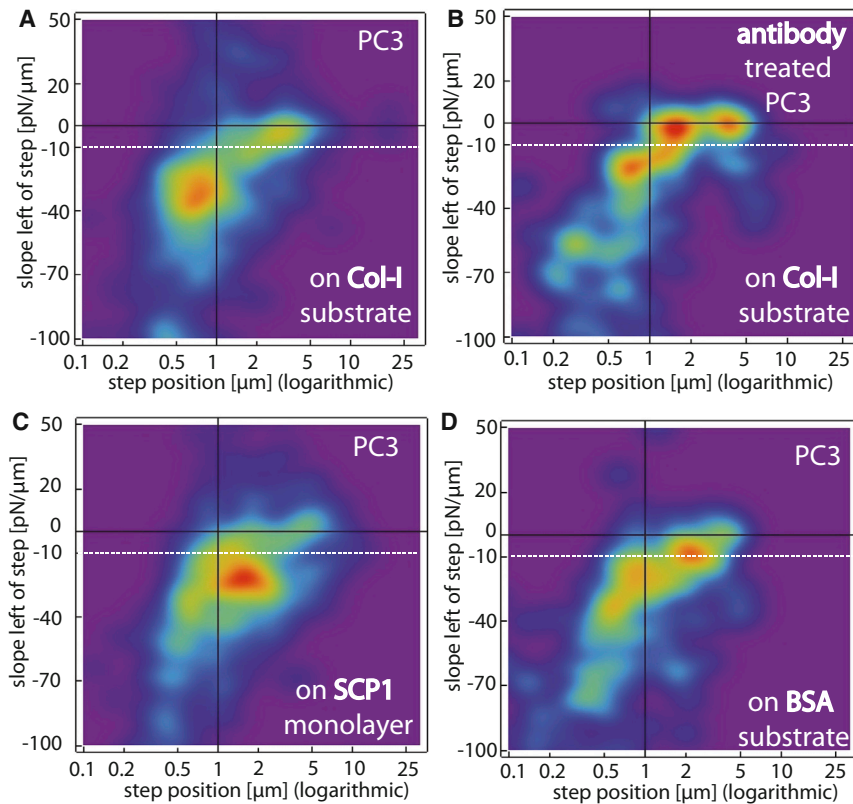


**FIGURE 3** Two-dimensional probability density plots of PC3 cells interacting specifically with Col-I (A) and SCP1 cells (C) and nonspecifically with BSA (D). (B) PC3 cells treated with monoclonal antibody to CD29/integrin  $\beta 1$  also interact nonspecifically with Col-I (see Fig. 2 D for color-coding of the probability densities). To see this figure in color, go online.

majority of interactions are clearly jumplike. If the PC3 cells are incubated with an anti- $\beta 1$  antibody (Fig. 3 B), the majority of interactions shift to the tether region of the plot. Similarly, if the cells are treated with latrunculin-A, a drug that disrupts the actin cytoskeleton by blocking G-actin, virtually all interactions are shifted to the tether region (see Fig. S1).

In contrast to the Col-I substrate, PC3 cells probed on the SCP1 substrate show fewer tethers and densely cumulate their jumplike steps at  $-30$  pN/ $\mu\text{m}$  and a distance of  $\sim 1.7$   $\mu\text{m}$ . This shift to higher step positions reflects the mechanical properties of the softer SCP1 cell layer compared to the stiff Col-I-coated substrate (compare the parts of Fig. 3, A and C). The reduced number of tethers indicates an increased coupling of receptors to the cytoskeleton on the SCP1 substrate compared to the collagen substrate. This may reflect an optimized accessibility of receptor-ligand pairs between interacting cells, as well as an effective suppression of nonspecific interactions compared to the collagen-coated glass substrates (12).

Finally, on BSA-coated substrates, the adhesion rate and number of steps is significantly lower (Fig. 2 A), as can be expected for a substrate allowing only nonspecific interactions. Accordingly, the initial jump population (Fig. 3 A) is shifted toward tethers, and only a few jumps remain (Fig. 3 D).

In summary, the slope position density plots help to visualize the embedding and anchorage of adhesion molecules in the cell. They reflect the substrate-dependent complex adhesion behavior of cells. In combination with results of

complementing techniques, such as quantitative polymerase chain reaction and blocking experiments, their readout allows identification of the specificity of the cellular interaction in the slope-position plane and strengthens the interpretation of single-cell force spectroscopy data, in particular with respect to the anchoring of the receptors in the cell.

## SUPPORTING MATERIAL

Supporting Materials and Methods and four figures are available at [http://www.biophysj.org/biophysj/supplemental/S0006-3495\(15\)00785-7](http://www.biophysj.org/biophysj/supplemental/S0006-3495(15)00785-7).

## AUTHOR CONTRIBUTIONS

E.S. performed the atomic-force-microscopy measurements and quantitative polymerase chain reaction work and evaluated the data together with J.P.M.; C.P. designed the quantitative polymerase chain reaction method and the cell treatments; D.D., H.C.-S., and M.B. designed the project and supervised the experiments; and H.C.-S. and M.B. wrote the article together with E.S.

## ACKNOWLEDGMENTS

We thank Erich Sackmann, Hermann Gaub, Stefanie Sudhop, and Michael Nash for helpful discussions, and Angelika Kardinal and Thomas Nicolaus for advice and support with the cell culturing.

We gratefully acknowledge financial support of the Ministry of National Education of Turkey, and of the German Excellence Initiative, via the Nanosystems Initiative Munich and the Deutsche Forschungsgemeinschaft.

## REFERENCES

1. Taubenberger, A. V., D. W. Huttmacher, and D. J. Muller. 2014. Single-cell force spectroscopy, an emerging tool to quantify cell adhesion to biomaterials. *Tissue Eng. Part B Rev.* 20:40–55.
2. Friedrichs, J., K. R. Legate, ..., M. Benoit. 2013. A practical guide to quantify cell adhesion using single-cell force spectroscopy. *Methods.* 60:169–178.
3. Celik, E., M. H. Faridi, ..., V. Gupta. 2013. Agonist leukadherin-1 increases CD11b/CD18-dependent adhesion via membrane tethers. *Biophys. J.* 105:2517–2527.
4. Lamontagne, C.-A., C. M. Cuerrier, and M. Grandbois. 2008. AFM as a tool to probe and manipulate cellular processes. *Pflug. Arch. Eur. J. Phys.* 456:61–70.
5. Helenius, J., C.-P. Heisenberg, ..., D. J. Muller. 2008. Single-cell force spectroscopy. *J. Cell Sci.* 121:1785–1791.
6. Sariisik, E., D. Docheva, ..., M. Benoit. 2013. Probing the interaction forces of prostate cancer cells with collagen I and bone marrow derived stem cells on the single cell level. *PLoS One.* 8:e57706.
7. Popov, C., T. Radic, ..., D. Docheva. 2011. Integrins  $\alpha2\beta1$  and  $\alpha11\beta1$  regulate the survival of mesenchymal stem cells on collagen I. *Cell Death Dis.* 2:e186.
8. Benoit, M., and C. Selhuber-Unkel. 2011. Measuring cell adhesion forces: theory and principles. *Methods Mol. Biol.* 736:355–377.
9. Benoit, M. 2010. Force spectroscopy on cells. In *Handbook of Nanophysics: Nanomedicine and Nanorobotics*. K. D. Sattler, editor. CRC Press, Boca Raton, FL 9:1–29.
10. Sun, M., J. S. Graham, ..., M. Grandbois. 2005. Multiple membrane tethers probed by atomic force microscopy. *Biophys. J.* 89:4320–4329.
11. Opfer, J., and K.-E. Gottschalk. 2012. Identifying discrete states of a biological system using a novel step detection algorithm. *PLoS One.* 7:e45896.
12. Chu, C., E. Celik, ..., V. T. Moy. 2013. Elongated membrane tethers, individually anchored by high affinity  $\alpha4\beta1$ /VCAM-1 complexes, are the quantal units of monocyte arrests. *PLoS One.* 8:e64187.

**Biophysical Journal**

**Supporting Material**

**Decoding Cytoskeleton-Anchored and Non-Anchored Receptors from Single-Cell Adhesion Force Data**

Ediz Sariisik,<sup>1,2,3</sup> Cvetan Popov,<sup>1</sup> Jochen P. Müller,<sup>2</sup> Denitsa Docheva,<sup>1,3</sup> Hauke Clausen-Schaumann,<sup>2,3</sup> and Martin Benoit<sup>2,3,\*</sup>

<sup>1</sup>Experimental Surgery and Regenerative Medicine, Department of Surgery and <sup>2</sup>Center for NanoScience, Ludwig-Maximilians-Universität München, Munich, Germany; and <sup>3</sup>Center for Applied Tissue Engineering and Regenerative Medicine, University of Applied Sciences, Munich, Germany

## SUPPLEMENTARY INFORMATION

### Materials and methods

#### Cell culture

PC3 were obtained from ATCC (Wesel, Germany). PC3 cells were maintained in RPMI-1640 cell culture media (PAA, Cölbe, Germany) and 10% FBS (Sigma-Aldrich, Munich, Germany). The immortalized human MSC line SCP1, which is fully described in Böcker et al (1), was cultured in MEM GlutaMAX culture media (Life Technologies, Karlsruhe, Germany) supplemented with 10% FBS. During routine cell culture, the two cell types were grown up to 80% confluency in a humidified incubator. Culture medium was changed three times per week and for cell passaging, cells were detached with 1x trypsin/EDTA solution (PAA).

#### Quantitative reverse transcriptase (RT)-PCR

Quantitative RT-PCR was performed as described in Popov et al (2). Briefly, total RNA was extracted from PC3 cells with RNeasy Mini Kit (Qiagen, Hilden, Germany). For cDNA synthesis, 1 µg total RNA and AMV First-Strand cDNA Synthesis Kit (Life technologies) were used. LightCycler Fast Start DNA Master SYBR Green kit (Roche, Munich, Germany) and primer kits for  $\alpha 1$ ,  $\alpha 2$ ,  $\alpha 11$ ,  $\beta 1$  and glyceraldehyde 3-phosphate dehydrogenase (GAPDH) (all Search-LC, Heidelberg, Germany) were applied. The PCR was performed in a LightCycler 1.5 instrument (Roche) equipped with LightCycler 3.5.3 software. Crossing points for each sample were determined by the second derivative maximum method and relative quantification was performed using the comparative  $\Delta\Delta C_t$  method according to the manufacturer's protocol. The relative gene expression was calculated as a ratio to GAPDH.

#### Substrate preparations

We used Col-I and bovine serum albumin (BSA)-coated glass cover slips and SCP1 monolayers as substrates for AFM force spectroscopy experiments. Sterile glass cover slips were coated with Col-I (100 µg/ml) or BSA (100 µg/ml) at 4 °C overnight. The full protocols used for the preparation of Col-I coated cover slips and SCP1 monolayers were described in Sariisik et al (3). Prior to use, the substrates were washed with and covered by 1.5 ml fresh serum-free MEM-Alpha medium supplemented with 15 mM Hepes. The Col-I and BSA coated cover slips were placed on top of the SCP1 monolayer in the culture dish lids. BSA coated glass cover slips were also used for cell capture.

### AFM setup and force spectroscopy

Fresh serum-free Alpha-MEM/Hepes medium was used as measurement media throughout all force spectroscopy experiments. The culture dish lid, containing BSA and Col-I coated substrate as well as the SCP-1 monolayer, was mounted on a temperature-controlled stage in the AFM and was left to equilibrate for 10 min at 37 °C. Force Spectroscopy experiments were conducted using a NanoWizard II with CellHesion module (JPK Instruments, Berlin, Germany), mounted on a Zeiss Axiovert-200-M (Carl Zeiss, Göttingen, Germany) with a custom made temperature unit. The force sensors used were tip-less silicon nitride cantilevers with a nominal spring constant of 0.01 N/m (Tipless, MLCT-O10, Veeco, USA). Prior to cell adhesion experiments, the force sensors were coated overnight with 100 mg/ml Poly D-Lysine (PDL, Millipore, USA). The spring constants of the force sensors were determined individually by the thermal noise method.

A single PC3 cell resting on the BSA coated cover slide was gently contacted for a few seconds by the PDL-coated tip-less force sensor and after lifting the attached cell it was allowed to firmly adhere to the force sensor for about 3 minutes. Subsequently, each substrate (BSA, Col-I and SCP1 in varied order) was contacted by this cell between 100 and 200 times for as short as possible (0.3 ms) at 100 pN. By scanning a list of 0.5 µm spaced points of preselected grids sampling repeatedly the same spot was avoided. Partially identical experiments with identical results (within the statistical error) were conducted in Sariisik et al (3). Therefore more detailed protocols and schematics of the experimental setup are given there.

Force-distance curves were recorded while the piezo traveled in a closed loop up to 20 µm at an approach velocity of 7 µm/s, until a trigger force of 100 pN was reached. Subsequently, the adhesion force signature was recorded at a retraction velocity of 3 µm/s.

#### Application of integrin blocking antibody

After detachment of PC3 cells, the released cells were collected and washed with PBS (lacking calcium and magnesium). Prior to force spectroscopy and cell adhesion measurements, PC3 cells were suspended with fresh serum-free culture medium supplemented with 15 mM Hepes (Sigma-Aldrich). A monoclonal antibody against CD29/Integrin  $\beta 1$  (Acris Antibodies, Inc. San Diego, CA USA, BM2540) in a concentration of 4.8 µg/ml was added into 0.5 ml cell suspension containing  $2 \times 10^5$  cells and incubated for 30 minutes at 37 °C in a humidified incubator.

### Latrunculin-A treatment of a cell on the cantilever (control experiment).

PC3 cells were prepared as described above for force spectroscopy experiments. One of the cells was captured from the BSA surface and attached to the PDL coated cantilever. Initially 60 force curves were collected on Col-I substrate with this cell, to check for normal adhesion properties (data not shown). (Subsequently Latrunculin-A (Lat-A, Sigma-Aldrich, USA) was added into the measurement medium until a final concentration of  $0.2 \mu\text{M}$  was reached. After a period of 15 minutes for allowing Lat-A to disrupt the actin cytoskeleton, 60 additional curves were recorded with the same cell. In total 4 different cells were treated and measured in this way.

### Force curve analysis

For data analysis, only the retraction part of the approach-retract cycles of the cell bearing cantilevers was evaluated (blue force traces in Fig. 1). In order to obtain characteristic quantitative information from the force-distance curves, a custom-designed data analysis and step detection software (4) was used to smooth the signal (black line on top of the blue line in Fig. 1), find the baseline (dashed lines in Fig. 1), correct for hydrodynamic drag and possible drift, and extract the following parameters (see also Sariisik et al (3)):

**step height** [pN] describing the difference in force measured before and after an individual detachment event, visible as a force step. The algorithm identifies such a step by maxima in the derivative of the smoothed signals, which surmount a certain threshold and marks it with a red cross (cf. also Fig. 1). Force steps smaller than 8 pN are not counted as steps.

**adhesion rate** [%] describing the fraction of curves with at least one detected force step.

**number of steps** describing the average number of steps detected per curve (only counting curves with at least one detected force step).

**step position** [ $\mu\text{m}$ ] describing the distance between the contact point (black circle at the intersection of baseline and force curve in Fig.1) and a force step.

**dissipated work** [aJ] describing the energy dissipated during that force experiment by integrating the area between baseline (zero force) and force curve. (Note, this has no trivial relation to the adhesion energy as, velocity dependent viscous and plastic deformation of

the cell and the cell membrane strongly contribute to the work of detachment)

**detachment force** [pN] describing the highest measured adhesion (global maximum) per curve.

We also analyzed force-loading rates (slope of the force trace) prior to each step by a line-fit to the force data points within the last 500 nm prior to the step. Due to the constant velocity of  $3 \mu\text{m/s}$  a loading rate [pN/s] could be directly derived from the force-distance trace.

In this study, we classified steep steps as **jump steps** at slopes below  $-10 \text{ pN}/\mu\text{m}$  ( $\sim$ loading rates of  $-30 \text{ pN/s}$  and steeper; Fig. 1A) and plateau steps as **tether steps** between slopes of  $\pm 10 \text{ pN}/\mu\text{m}$  ( $\sim$ loading rates between  $\pm 30 \text{ pN/s}$ ) see Fig. 1B and Fig. 2C&D).

For illustrating the advantage of the 2D-plots, the fraction of steps originated from tethers -as selected by eye in the classic manner- were marked in grey in the histogram of Fig 2C. According to this histogram, there is an area between  $-8$  and  $-14 \text{ pN}/\mu\text{m}$  where jumps and tethers are not clearly discernible by their slope.

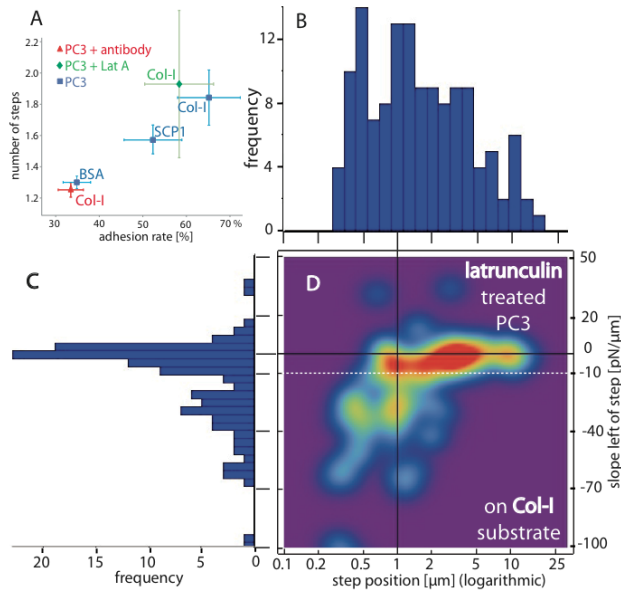
At the slope of  $-10 \text{ pN}/\mu\text{m}$  we chose to set a guiding line for separating between tethers and jumps in case for the PC3 cell line studied here. Note that the values of the slopes may vary between different cell types and that cells are visco-elastic objects. Therefore, the slopes of jumps will depend on the cantilever velocity (in this study the velocity was  $3 \mu\text{m/s}$ ).

Note, that the fit range of 500 nm for analyzing the slopes is a compromise between a reliable fit range to cope with the intrinsic noise of the force curves and the distance between individual steps. In case of steps closer than 500 nm in distance the algorithm detecting the slopes prior to each step generates positive slopes even larger than the noise level of about  $-10 \text{ pN}/\mu\text{m}$  by fitting through more than one step. Such positive slopes larger than  $+10 \text{ pN}/\mu\text{m}$  are therefore neglected when interpreting the density plots.

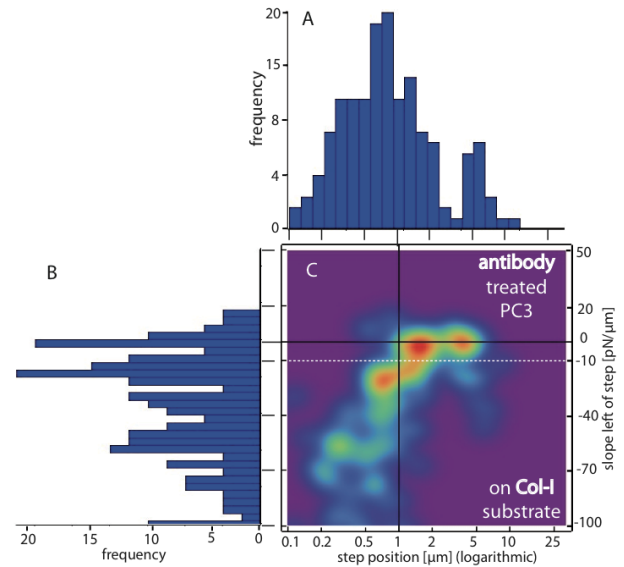
### Preparation of 2D density plots

The slope versus peak position 2D density plots were smoothed using a Gaussian kernel density estimation ( $\sigma_x = \log(x) \cdot 0,1 \mu\text{m}$   $\sigma_y = 5 \text{ pN}/\mu\text{m}$ ) for better visualization of the otherwise checkerboard patterned 2D-histograms. The density plots were normalized in order to compare tethers and jumps in the different experiments, i.e. on the different substrates.

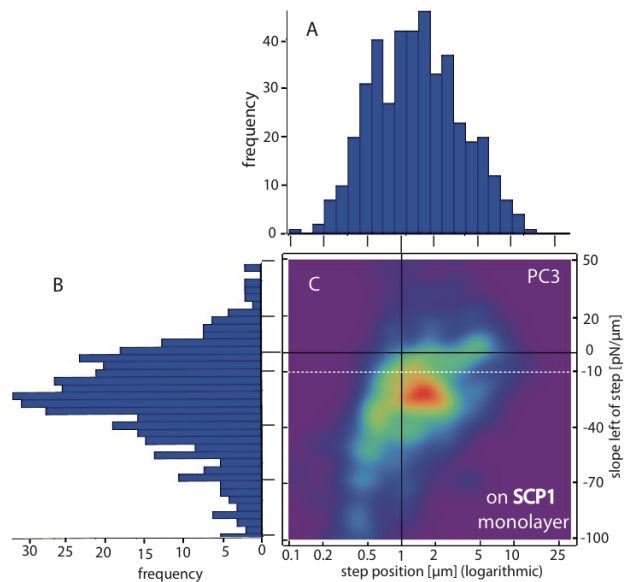
Supplementary Data



**Supplementary figure 1:** Adhesion rate vs. number of steps (A), histograms (B, C), and density plot (D) of latrunculin-A treated cells. In the adhesion rate vs. number of steps plot (A), the Lat-A treated cells appear in a similar range as the untreated cells, as the type of interaction is not changed but only the anchoring to the cytoskeleton is affected. Due to the smaller number of experiments (4 cells were measured instead of 10), the error bars are larger. The histogram of the position (B) shows a broad distribution with a maximum above 1 μm. The histogram of the slopes (C) shows a prominent peak close to 0 pN/μm indicating that the receptors are anchored predominately via membrane tethers, as expected for a disrupted cytoskeleton when only the cell membrane can anchor the interacting cell surface receptors. The density plot (D) clearly visualizes this broad distribution of mainly tethers (Note that the color code is identical to Fig 2 D; black lines mark “1 μm” and “0 pN/μm” slope, whereas the white dotted line marks “-10 pN/μm” as guide for the eye to separate tethers from jumps).



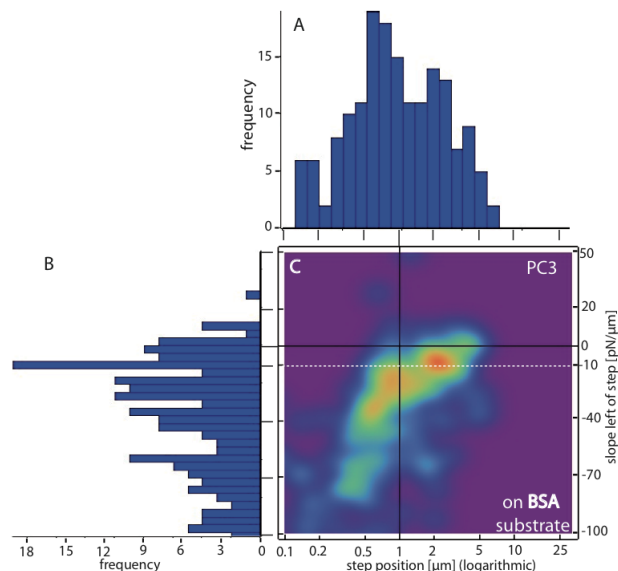
**Supplementary figure 2:** histograms behind the density plot of Figure 3B. The histogram of the position (A) shows one peak below 1 μm and a smaller peak above 3 μm. The histogram of the slopes (B) shows a two peaks close to 0 pN/μm and -20 pN/μm respectively. Due to the low adhesion rate the absolute number of points is small. The density plot (C) reveals a concentration of interactions to the tether region, but not as completely as Lat A. (The color code is identical to Fig 2 D; black lines mark “1 μm” and “0 pN/μm” slope, the white dotted line marks “-10 pN/μm” as guide for the eye to separate tethers from jumps)



**Supplementary figure 3:** histograms behind the density plot of Figure 3C. The histogram of the position (A) shows a broad distribution (similar to Lat-A treated



cells in Figure S1) with a maximum above  $1\ \mu\text{m}$ . The histogram of the slopes (B) shows a broad maximum close to  $-30\ \text{pN}/\mu\text{m}$ . The density plot (C) shows a concentration of all interactions in the region marked with the white dotted circle, which is shifted from below  $1\ \mu\text{m}$  in the case of collagen substrate (figure 2C) to values above  $1\ \mu\text{m}$  here. (The color code is identical to Fig 2 D; black lines mark " $1\ \mu\text{m}$ " and " $0\ \text{pN}/\mu\text{m}$ " slope, the white dotted line marks " $-10\ \text{pN}/\mu\text{m}$ " as guide for the eye to separate tethers from jumps)



**Supplementary figure 4:** histograms behind the density plot of Figure 3D. The histogram of the position (A) shows a broad distribution with one maximum below  $1\ \mu\text{m}$  and a weaker one above  $2\ \mu\text{m}$  (not as separated as in Fig S2). The histogram of the slopes (B) shows a broad distribution with a peak at  $-10\ \text{pN}/\mu\text{m}$ . Due to the low adhesion rate, the absolute number of points is small. The density plot (C) shows a concentration of most interactions in the tether region with some short ranged interactions. (The color code is identical to Fig 2D; black lines mark " $1\ \mu\text{m}$ " and " $0\ \text{pN}/\mu\text{m}$ " slope, the white dotted line marks " $-10\ \text{pN}/\mu\text{m}$ " as guide for the eye to separate tethers from jumps)

### Step position and bond lifetime

At constant pulling velocity, the length of membrane tethers directly correlates to the lifetime of the bond(s) that led to the pulling of tethers. Unfortunately, in many cases, only the step position can be unambiguously extracted from the force curves; in the case of multiple tethers pulled or tethers originating from a preexisting

filopodium, the tether-length does not necessarily coincide with the step position. To avoid over- or misinterpretations, we recommend thorough analysis of the datasets for those steps, where the step positions coincides with the true tether-length, whenever the bond lifetimes under force are in the focus of the investigation.

### REFERENCES

1. Böcker, W., Z. Yin, I. Drosse, F. Haasters, O. Rossmann, M. Wierer, C. Popov, M. Locher, W. Mutschler, D. Docheva, and M. Schieker. 2008. Introducing a single-cell-derived human mesenchymal stem cell line expressing hTERT after lentiviral gene transfer. *J. Cell. Mol. Med.* 12: 1347–1359.
2. Popov, C., T. Radic, F. Haasters, W.C. Prall, A. Aszodi, D. Gullberg, M. Schieker, and D. Docheva. 2011. Integrins  $\alpha2\beta1$  and  $\alpha11\beta1$  regulate the survival of mesenchymal stem cells on collagen I. *Cell Death Dis.* 2: e186.
3. Sariisik, E., D. Docheva, D. Padula, C. Popov, J. Opfer, M. Schieker, H. Clausen-Schaumann, and M. Benoit. 2013. Probing the Interaction Forces of Prostate Cancer Cells with Collagen I and Bone Marrow Derived Stem Cells on the Single Cell Level. *PLoS ONE.* 8: e57706.
4. Opfer, J., and K.-E. Gottschalk. 2012. Identifying Discrete States of a Biological System Using a Novel Step Detection Algorithm. *PLoS ONE.* 7: e45896.